Article

AquaCrop Simulation of Winter Wheat under Different N Management Practices

Nicholas Dercas [1,*], Nicolas R. Dalezios [2], Stamatis Stamatiadis [3], Eleftherios Evangelou [4], Antonios Glampedakis [5], Georgios Mantonanakis [1] and Nicholaos Tserlikakis [1]

[1] Laboratory of Agricultural Hydraulics, Department of Natural Resources Development and Agricultural Engineering, Faculty of Environment and Agricultural Engineering, Agricultural University of Athens, 75 Iera Odos Str., 11855 Athens, Greece; georgios_madonanakis@hotmail.com (G.M.); nikolastserlikakis@gmail.com (N.T.)

[2] Laboratory of Hydrology and Aquatic Systems Department of Civil Engineering, Faculty of Engineering, University of Thessaly, 38334 Volos, Greece; dalezios.n.r@gmail.com

[3] Goulandris Natural History Museum, Soil Ecology and Biotechnology Laboratory, 13 Levidou Str., 14562 Kifissia, Greece; stam@gnhm.gr

[4] Institute of Industrial and Forage Crops, Hellenic Agricultural Organization "Demeter", 1 Theophrastos Str., 41335 Larisa, Greece; levagel@gmail.com

[5] Red Coast International, Sergey Rumyantsev Str., 2700 Blagoevgrad, Bulgaria; antonis_glamb@yahoo.gr

* Correspondence: ndercas1@aua.gr

Abstract: AquaCrop is a well-known water-oriented crop model. The model has been often used to simulate various crops and the water balance in the field under different irrigation treatments, but studies that relate AquaCrop to fertilization are rare. In this study, the ability of this model to simulate yield and the water balance parameters was investigated in a wheat field under different nitrogen management practices. During the 2015–2016 and 2016–2017 growing seasons, meteorological data were provided from a nearby meteorological station, and the evolution of soil water content and final yields were recorded. The model showed a very good performance at simulating the soil water content evolution in the root zone. Notwithstanding its simplicity, AquaCrop based on a semi-quantitative approach for fertility performed well at the field level for the final yield estimation under different nitrogen treatments and field topography variation. Although the correlation coefficient between simulated and measured final yields was high, increased values of variations were observed in the various zones of this experimental field (−50% to +140%). The model appears to be an efficient tool for evaluating and improving the management practices at the field level. The experiments were conducted in Thessaly, which is the largest plain and the main agricultural area of Greece. Thessaly, however, has a strong negative water balance, which has led to a strong decrease in the level of the aquifer and, at the same time, to sea intrusion. There is also a significant risk of contamination of the groundwater aquifer due to increased use of agrochemicals. This analysis is particularly important for Thessaly due to the need for improvement of agricultural practices in this area, to decrease the pressure of agricultural activities on natural resources (soil, water) and reverse the consequences of current management.

Keywords: wheat; nitrogen management; AquaCrop model

1. Introduction

The winter and spring rainy seasons are the periods of wheat cultivation in Greece [1] with the possible water surplus drained or running off the farms. Some farmers apply supplementary irrigation in the spring that is usually not scheduled properly [2]. To reduce water losses and nitrogen leaching, a crop simulation model is needed that is able to combine the available field data, i.e., temperature, rain/irrigation, soil texture, and dry yield. Based on the concept of a direct link between crop water use and crop yield [3], the

AquaCrop model estimates biomass production directly from actual transpiration through a water productivity parameter. A linear relationship between crop transpiration and biomass production [4] was assumed by AquaCrop that adopts a water-driven strategy. AquaCrop was selected for its ability to predict crop productivity, water requirement, and water use efficiency under unstressed conditions [5], as well as conditions limited by water or fertility stress [6–14]. As mentioned above in Thessaly where the study was carried out, the water factor is in crisis. It is also well known that any study of nitrogen fertilization must take into account the water as nitrates are highly agile and contaminate aquifers and adjacent streams. Thus, a simulation program with dual targeting is necessary. Our target is to evaluate the possibilities of AquaCrop to satisfy such studies with sufficient accuracy. It is a multi-crop model able to simulate the yield of herbaceous crop types under different biophysical and management conditions [15,16]. It requires a relatively small number of explicit and mostly intuitive parameters to be defined compared to other crop models and has been validated and applied successfully for multiple crop types across a wide range of environmental and agronomic settings (for a recent review, see [17]).

The effects of soil fertility and salinity stresses are also considered indirectly by the model based on local calibration to relative biomass under different fertility and salinity conditions.

AquaCrop has also been amended with and evaluated for crop responses to atmospheric [CO_2] [18] and can be used for climate impact studies [17,19–21]. With less input information than Crop-Syst and WOFOST, AquaCrop performs similarly in simulating both biomass and yield at harvesting [13]. Model calibration for the local environment is very important for accurate prediction and sustainable management. AquaCrop has been tested for different crops under different hydro-meteorological conditions worldwide, for example, potato [21], sunflower [13,22], tomato [23], cotton [6,7,24], maize [10,11,22,25–28], quinoa [8,9], sugar beet [22], barley [29], tef [30,31], rice [12], soybean [32,33], and wheat [5,26,27,34–41]. All these investigations have reported that the AquaCrop model is able to simulate the crop biomass (B), grain yield (GY), canopy cover (CC), and soil water content accurately under different irrigation and fertility conditions.

The model has also been validated in Southern Africa [42], Eastern Africa [43–45], and West Africa [46]. These studies showed that the model could satisfactorily simulate crop yield and biomass, as well as soil water productivity under rainfed, full and deficit irrigation, and soil fertility stress [45,46].

The productive portion of water consumption (i.e., transpiration) estimates biomass accumulated each day, using a crop-specific water productivity parameter that is normalized for reference evapotranspiration [4], making the parameter applicable to a wide range of climates. Subsequently, the proportion of biomass that becomes harvestable yield is calculated using a harvest index parameter that increases over the growing season and responds to water and temperature stresses. Steduto et al., (2009) [16] contains a very comprehensive description of the model's conceptual design.

AquaCrop is distinguished from other crop models by several unique features. First, canopy expansion is simulated in terms of proportional green canopy cover as opposed to leaf area index. This approach has the advantage that simulated model outputs can be related directly to easily accessible data from visual field observations and remote sensing, i.e., vegetation indices obtained from satellite images.

A major limitation of the model is that pests and diseases are not considered, which at times can lead to crop yield over-estimation. Additionally, the model has been shown to produce poor estimates under severe water-stress treatments especially during senescence [10].

This study investigated the ability of the AquaCrop model to simulate the water balance parameters of winter wheat under different nitrogen (N) management practices. These included variable rate application (VRA) using a sensor-based model to calculate spatially adjusted N rates on-the-go [47]. Compared to the conventional uniform practice,

the in-season VRA approach significantly reduced N inputs without yield losses in winter wheat, thus offering higher revenue over fertilizer costs with the least uncertainty to the farmer [40]. However, VRA systems are effective when N does not escape from the rooting zone after fertilizer has been applied. Furthermore, N leaching raises environmental concerns in areas of intensive cultivation. European Union member countries are obliged to comply with the Water Directive (2000/60/CE) [48] that requires countermeasures for N water pollution. For these reasons (economic and environmental), synchronization of fertilization with the water cycle variability is the suitable strategy [49].

The objectives of this study were: (i) evaluation of the effectiveness of AquaCrop to estimate the soil water content evolution and water balance in the field and (ii) calibration and validation of the model to simulate winter wheat yield under various N treatments.

2. Materials and Methods

2.1. Field Experiments and Data

The field experiments were carried out in a winter wheat field near the village of Nea Lefki (Larisa, central Greece) at the coordinates of 39°31′30″ N, 22°30′52″ E and an altitude of 125 m [50,51]. The temperate Mediterranean climate has cold humid winters but hot and arid summers (Bsk—Csa according to Köppen's climatic classification) [1]. Based on historical data, the mean minimum and maximum temperatures are 0.5 °C (January) and 33 °C (July), respectively, with an average relative humidity of 67%. The mean monthly rainfall varies from 15.5 mm (August) to 58.2 mm (November) with a mean annual total of 313 mm. During the November to May growing season, the mean total rainfall is 277 mm, and the average monthly temperature varies from 5 °C in January to 17 °C in May [51]. The rainfall was 255.0 mm and 283.8 mm during 2015–2016 and 2016–2017 growing seasons, respectively.

A soil sampling was performed with regard to field topography, at lower, middle, and upper zones of the field. A composite soil sample (0–20 and 20–40 cm depth, n = 3) was collected from 1 m^2 sub-plots in three landscape positions of each treatment strip (lower zone, middle zone, and upland zone). Soil samples were analyzed in the laboratory for soil texture as determined by physical fractionation (Bouyoukos 1951) [52], and for soil organic matter as determined by the Walkley–Black method of wet oxidation [53]. Carbonate content, as an estimate of inorganic C, was determined by using a Bernard calcimeter to measure the released carbon dioxide (CO_2) after addition of dilute hydrochloric acid (HCl) solution [53]. Total N was measured by the semimicro-Kjeldahl method [54]. Soil K was extracted with 1 N ammonium acetate at pH 7 [55] and measured by a Corning 410 flame photometer. Available P was determined as per Olsen and Sommers (1982) [56].

The soil in the field is classified as a Vertic Xerochrept of clay-to-clay loam texture, but with differences in the soil properties relevant to topography (Table 1).

Strong effects of soil erosion in the slopes and upland areas of the field have been reported by Stamatiadis et al. (2018) [50]. Those areas of the field had a higher carbonate and lower organic matter and total N content than the lowland plots as a result of the removal of surface horizons that revealed the parent material rich in calcium carbonate.

The topographic variation in the field is shown in Figures 1 and 2. The lower ground level on the slope by 1–2 m, relative to the adjacent field on the right (Figure 1, see the red arrow), appears to be the product of soil erosion. In contrast to the adjacent field, winter wheat was grown without rotation over recent decades. The soil properties in different sections of the field were analyzed in the laboratory.

The grown wheat cultivar was Simeto, an Italian variety that is popular among Greek farmers. This cultivar was selected based on its high yield, climatic adaptability, and performance stability. Seeds were sawn at a density of 270 kg/ha on 21 November 2015 and on 26 November 2016. Supplementary irrigation was applied in all plots: 68 mm in May 2016 and 56 mm in May 2017. The grain was harvested on 5 June 2016 and 10 June 2017, respectively.

Table 1. Soil properties by landscape position (n = 12).

| Soil Depths (cm)	Soil Properties	Landscape Position		
		Lower Zone	Middle Zone ZoneSlope	Upper Zone Land
0–20	Sand (%)	38.0	43.8	34.3
	Clay (%)	44.4	36.3	46.7
	Silt (%)	17.6	19.9	19.1
	SOM (%)	2.02	1.44	1.87
	$CaCO_3$ (%)	5.4	26.3	35.2
	Total N (%)	0.122	0.095	0.107
	P-Olsen (mg/kg)	7.54	5.68	8.00
	K (cmol/kg)	0.80	0.44	0.48
20–40	Sand (%)	40.1	47.9	31.4
	Clay (%)	42.1	35.4	48.5
	Silt (%)	17.8	16.7	19.8
	SOM (%)	1.68	1.29	1.60
	$CaCO_3$ (%)	5.1	24.5	41.5
	Total N (%)	0.108	0.087	0.098
	P-Olsen (mg/kg)	3.69	3.53	5.38
	K (cmol/kg)	0.65	0.39	0.39

**Figure 1.** Side view of the experimental field.
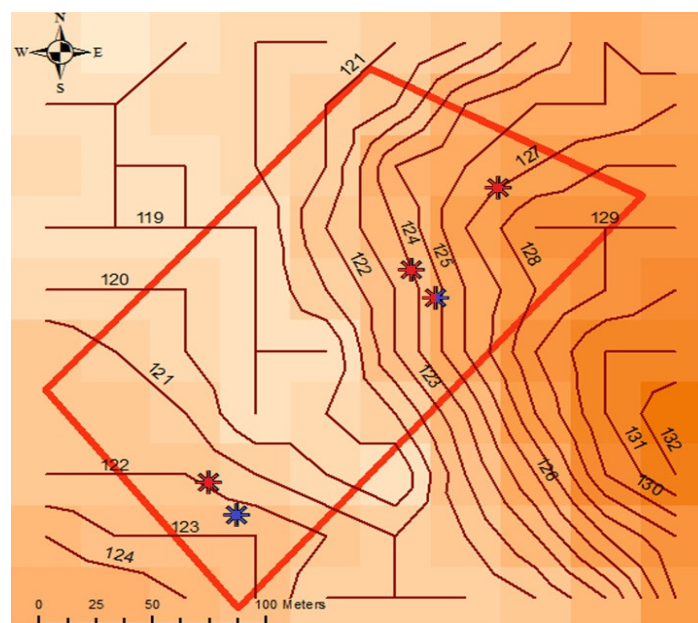
Figure 2. Topographic map of the field (source: Open Topography). (Blue star, 2015–2016; red stars, 2016–2017; red/blue, star both growing seasons.).

The field was divided into four blocks, and three N treatments were randomly assigned within each block to follow a randomized complete block design (Figure 3). Each treatment was a field strip of 7 m wide running the entire length of the field (200 m) to simulate full-scale field conditions. The three treatments during the 2015–2016 growing season consisted of preplant application only (100 kg N/ha), a farmer preplant and in-season uniform N application (100 + 112 kg N/ha), and a preplant with in-season VRA (100 + VRA kg N/ha). During the 2016–2017 growing season, the farmer rates were reduced so the respective treatments were the preplant (50 kg N/ha), the farmer application (50 + 100 kg N/ha), and the VRA treatment (50 + VRA kg N/ha).
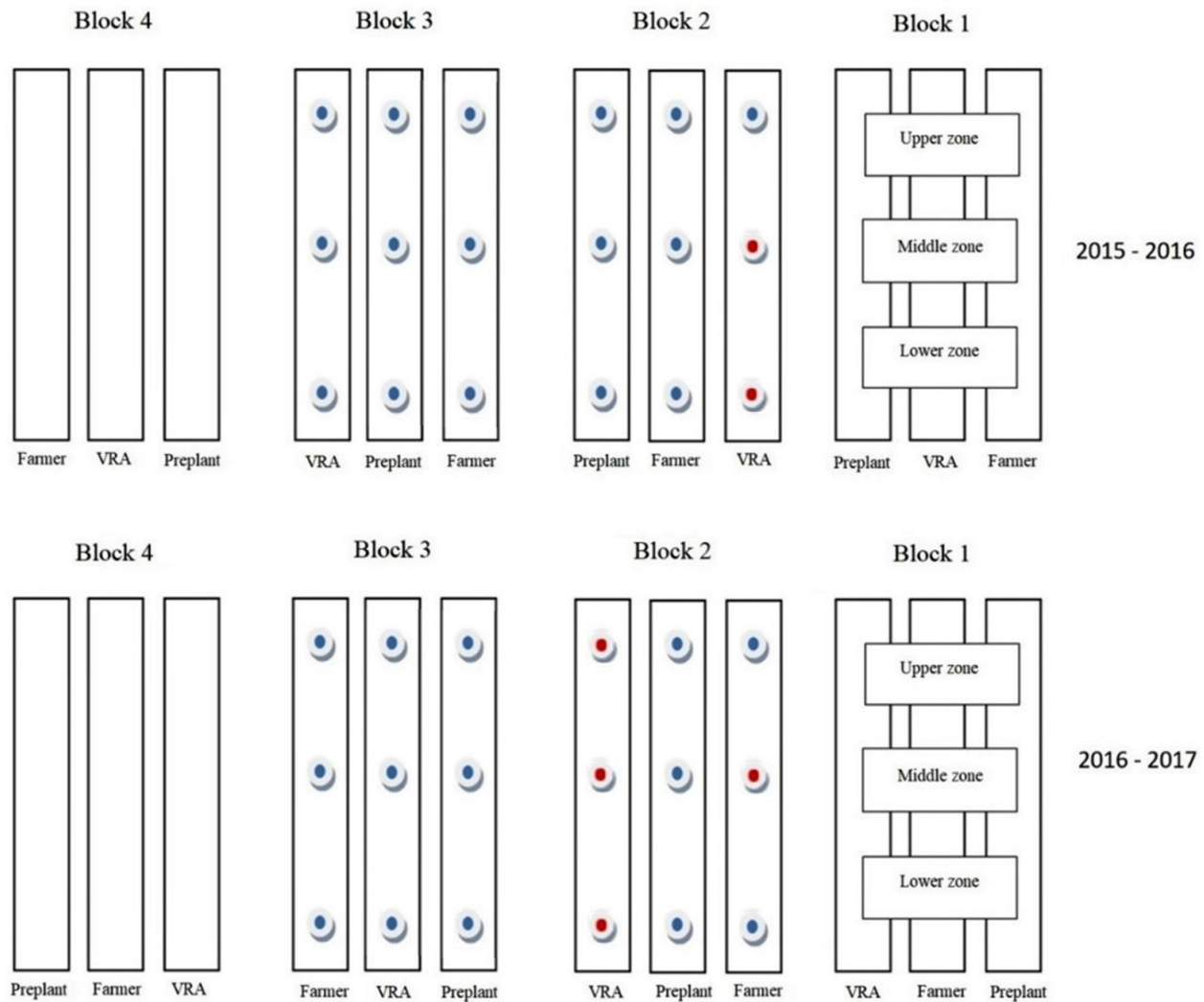
Figure 3. Experimental design for 2015–2016 and 2016–2017 growing seasons. Blue points represent a soil moisture sensor at 30 cm depth. Red points represent a station of five soil moisture sensors monitoring 1 m depth.

Figure 4a shows the average daily temperatures for the two growing seasons, as well as the monthly average of a thirty-year period from the CLIMWAT base [57]. The data allowed us to assess whether the temperature conditions of the two experimentation years are close to those of an average year. Figure 4b shows the daily rainfall during the two growing seasons. Average daily temperatures and daily rainfall are inputs for Aqua Crop. Figure 4c shows the monthly rainfall of the two growing seasons and the average monthly rainfall of a thirty-year period from the CLIMWAT database [57]. These data allowed us to assess whether the rainfall conditions of the two experimentation years are close to those of an average year.
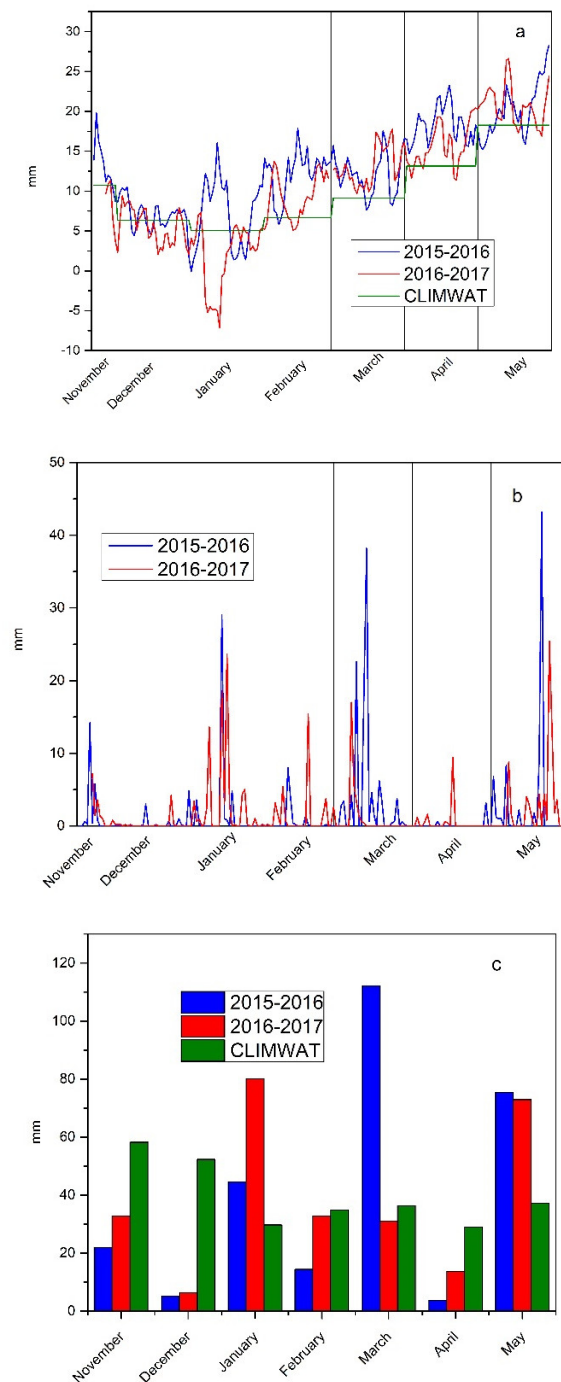
Figure 4. (**a**) Mean temperature of 2015–2016 and 2016–2017 growing seasons compared to 30 years average temperature according to FAO database/CLIMWAT, Larissa area [57]. (**b**) Comparison of 2015–16 and 2016–17 precipitation. (**c**) Comparison of 2015–2016 and 2016–2017 monthly precipitation to FAO database/CLIMWAT, Larissa area [57].

2.2. Soil Moisture Measurement Network

EM50 and Em50b data loggers and EC5 and 10HS soil moisture capacitance sensors (Decagon devices, 2365 NE Hopkins Ct, Pullman, WA 99163, USA) were used to dynamically monitor the soil water content during the growing season at different field positions. Based on topographic features, the experimental field was divided into a lower, a middle, and an upper zone. Each zone of the field was equipped with soil moisture sensors installed at a 30 cm depth in the treatment strips of the two central blocks in the fall of 2015. One additional multi-sensor system (with 10HS sensors) was installed at 10, 30, 50, 70, and

90 cm depths in the lower and middle zone of block 2 to monitor the soil moisture of the 1 m profile. Their exact position is shown with the star symbols of Figure 2. A similar arrangement was followed in the fall of 2016, but with four multi-sensor systems to cover all topographic zones. To improve the accuracy of soil moisture sensors, a specific calibration was carried out for the soil conditions of the experimental field.

The sensors were installed in a horizontal position a few days after sowing and the soil water content was measured every 2 h. Disturbed and undisturbed soil samples were taken from the trenches for texture, gravimetric soil moisture, and bulk density determination. To minimize disturbance to the soil structure during 10HS-sensor installation, the soil was excavated layer by layer and was backfilled in its place. The soil was then thoroughly compacted to make good contact with the sensors and restored to its natural density. The good sensor–soil contact was checked with a ProCheck device (Decagon, USA). New grain was sown at the surface to restore plants that were removed. Sensors were installed at a 30 cm soil depth (EC5 sensors) because a previous analysis [58] showed that the measurement at this depth is a good approximation of the average moisture of the 0–100 cm layer.

2.3. AquaCrop Model Description

AquaCrop was designed as an evolution from the original FAO Irrigation Drainage Paper 33 [3], which represents the yield response to water as a linear, crop-specific function of the ratio of actual to potential evapotranspiration over a growing season. Steduto et al., 2009 [16] contains a very comprehensive description of the model's conceptual design.

AquaCrop simulates soil water balance and crop growth processes as a function of crop, soil, weather, and management input data on a daily time step [59]. In addition, AquaCrop simulates soil evaporation and crop transpiration explicitly as individual processes. Crop yield response is understood as a function of water consumption [60]. The calculation cycle contains a simulation of green canopy development (CC), crop transpiration (Tr), aboveground biomass production (B), and crop yield [60,61]. AquaCrop has four sub-model components: (i) the soil (water balance); (ii) the crop (development, growth, and yield); (iii) the atmosphere (temperature, rainfall, evapotranspiration (ET), and carbon dioxide (CO_2) concentration); and (iv) the management (major agronomic practices such as planting dates, fertilizer application, and irrigation if any) [35].

The AquaCrop model is a water-driven model because it simulates aboveground biomass production in exchange for water transpired by the crop according to the following relation [16,19]:

$$B_n = WP^* \times \sum_{i=1}^{n} \left(\frac{Tr_i}{ETo_i} \right) \tag{1}$$

where B_n is the cumulative aboveground biomass produced after n days (g m^{-2}); Tr_i is the crop transpiration per day (mm day^{-1}); ETo_i is the daily reference evapotranspiration (mm day^{-1}); $i = 1 \ldots n$ are the days for B_n production; WP^* is the normalized crop water productivity (g m^{-2}).

The crop canopy development and phenology are driven by temperature. The water transpired by the crop is determined by the canopy cover [19].

It also simulates daily water movement in and out of the soil profile considering surface runoff, infiltration, capillary rise, soil evaporation, and crop transpiration. As for water balance, the simulation starts with the drainage of the soil profile. Subsequently, water infiltrates into the soil profile (after the subtraction of surface runoff) or moves upward by capillary rise from a shallow groundwater table. Finally, the amount of water lost by soil evaporation and crop transpiration is calculated. In each of the described subroutines, the soil water content is updated at the end of the time step and at each soil layer, resulting in the final daily water content [61]. When calculating the soil–water balance, the amount of water stored in the root zone can be expressed as an equivalent water depth (Wr) or as root zone depletion [2]. This allows the calibration and validation of the model with soil moisture measurements taken in the field.

Unlike all other models, AquaCrop uses canopy cover (CC), not leaf area index (LAI). The use of CC, as opposed to LAI, is meant to introduce simplicity by reducing the overall aboveground growth into just a single growth function [62].

AquaCrop does not explicitly consider nutrient cycles or balances [46,60]. However, soil fertility stress is determined by its expected effect on crop biomass production, using a semi-quantitative assessment to establish the degree of stress resulting from various levels of nutrient deficiency. Under these conditions, the model is based on local calibration to relative biomass under different fertility and salinity conditions. This approach yields a ratio (Brel), calculated as the total dry aboveground biomass at the end of the growing season in a field with soil fertility stress (Bstress) divided by that without soil fertility stress (Bref) (see Equation (2) and [37]).

$$Brel = Bstress/Bref \times 100\% \qquad (2)$$

As shown in Equation (2), Brel ranges from 0%, meaning complete crop failure from nutrient deficiency, to 100%, indicating no nutrient stress. This characteristic of the model allows the user to simulate the combined effect of soil fertility and water stress that is a major strength of the model [46]. Using Bref, harvest index, and Brel, the final yield is estimated.

2.4. Simulation Procedure

(i) The evaluation aimed at the effectiveness of AquaCrop to simulate the soil water content evolution and crop yield in different areas of an experimental field under different treatments. Two soil water content profiles (up to 1 m depth) in the 2015–2016 growing season and four profiles in the 2016–2017 growing season were used (Figure 3). Table 2 present the conservative and the nonconservative parameters used for the simulations during the two growing seasons. The model was adjusted to crop yield (kg/ha) as measured in plot samples. Measurement of soil water content is a prerequisite for establishing a reliable water balance at the field scale.

(ii) AquaCrop was evaluated to estimate the wheat yield under different treatments. The simulation was a two-step procedure: (a) simulations at field positions with 30 cm soil moisture sensors (blocks/repetitions 2 and 3) were used to determine soil water content evolution, yield, and average fertility per zone and treatment (**Calibration of the model**); (b) using these fertility levels and local soil data, crop production was estimated in other parts of the field with available yield data (blocks/repetitions 1 and 4) under different N treatments. The simulated yields were compared to the field yields (**Validation of the model**). For the simulation, we used the default in the AquaCrop wheat.cro file (Valenzano).

For the two cultivation periods, the reference evapotranspiration was calculated by the model using as input the minimum, mean, and maximum daily temperature according to FAO 56 protocol [63]. For this evaluation, data from a private database (larisa.meteoclub.gr) were used. For comparative reasons, the mean reference annual evapotranspiration was presented using 30 year data from the FAO database concerning the region of Larissa (near the study area). The CROPWAT model was used for the 30 year average ETo. Meteorological data were provided by CLIMWAT [57].

The physical soil characteristics of all the plots in the upper, lower, and middle zone of the experimental field were determined. They were processed with Soil Water Hydraulic Properties Calculator [64] to calculate hydraulic parameters required by AquaCrop. These included volumetric soil water content at field capacity (FC), permanent wilting point (PWP), saturation (SAT), and saturated hydraulic conductivity (Ksat). Curve number was also adjusted to slope variations according to the Sharply–Williams method [65].

Table 2. Conservative and Fine-tuned non-conservative crop parameters used for AquaCrop.

A. Conservative Crop Parameters	
Base temperature (°C) below which crop development does not progress	0.0
Upper temperature (°C) above which crop development no longer increases with an increase in temperature	26.0
Crop coefficient when canopy is complete but prior to senescence (KcTr, x)	1.10
Water productivity normalized for ETo and CO_2 (WP*) (g/m^2)	15.0
Possible increase (%) in HI due to water stress before flowering	5
Coefficient describing positive impact on HI of restricted vegetative growth during yield formation	10.0
Coefficient describing negative impact on HI of stomatal closure during yield formation	7.0
Allowable maximum increase (%) in specified HI	15
Soil water depletion factor for canopy expansion (p-exp)—Upper threshold	0.20
Soil water depletion factor for canopy expansion (p-exp)—Lower threshold	0.65
Soil water depletion fraction for stomatal control (p-sto)—Upper threshold	0.65
Soil water depletion factor for canopy senescence (p-sen)—Upper threshold	0.70
Minimum growing degrees required for full crop transpiration (°C—day)	14.0
B. Fine-Tuned Non-conservative Parameters	
Number of Plants per Hectare	185,000
Degree Days: from sowing to emergence	150
Degree Days: from sowing to max. canopy	1186
Degree Days: from sowing to flowering	1250
Degree Days: from sowing to senescence	1700
Degree Days: from sowing to maturity	2400
Maximum canopy cover (CCx) in fraction soil cover	0.96
Maximum effective rooting depth (m)	1.00
Average root zone expansion (cm/day)	0.9
Reference Harvest Index (HIo) (%)	48

3. Results

3.1. Meteorological and Soil Conditions

The reference evapotranspiration was close to the 30 year average in both years of the experiment (Figure 5). This was not the case with rainfall (Figure 4c) and the mean air temperature (Figure 4a). During March and May 2016, the rainfall events were close or higher than 40 mm (Figure 4b). Monthly precipitation was higher than the 30 year average during March 2016, and January and May 2016 and 2017. On the contrary, during December and April of both growing seasons, the monthly rainfall was much lower than the 30 year average.

Soil texture was significantly affected by the topographic variation. The slope had coarser soil due to erosion that lowered the level of the ground (see photo in Figure 1) as a result of management practices and crop rotations.

The soil texture analysis indicated the high spatial variability of the experimental field (Table 3). The lower zone had a predominantly clay texture. The upper zone also had a clay texture (C), but some positions were characterized as clay loam (CL) and two positions with increased sand (sandy clay (SC), in Blocks 1 and 3). Due to slope, the soil of the middle zone was eroded so that SC and sandy clay loam (SCL) were often present. Only the left of the experimental field (Block 4) had reduced erosion due to the lower slope, and class C was the main soil texture.

Wilting point and field capacity were determined using soil texture at the sampling points and Soil Water Hydraulic Properties Calculator [51]. Their values were higher in the lowland area due to the increased fine particles (clay and silt).

3.2. Simulation: Model Calibration and Validation

The model was adjusted to the measured plot yields where the 1 m soil moisture profile was installed (Table 4). The water balance was calculated for the same plots (Table 5). Figure 6 presents the measured and simulated 1 m soil water content during the growing season. Their correlation coefficients are shown in Table 5 (n = 87). For the estimation of water content in the root zone, data of five soil moisture sensors per profile were used.
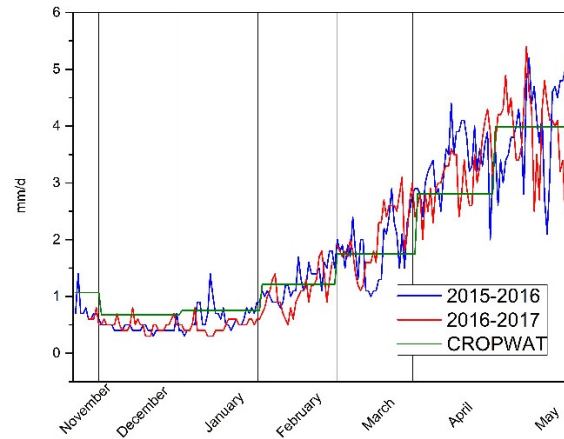

Figure 5. The reference evapotranspiration for 2015–2016 and 2016–2017 cultivation periods compared to the 30 year average ETo according to FAO database/CLIMWAT, Larissa region.

Table 3. Soil texture analysis of the experimental plots (0–20 cm and 20–40 cm) (*).

Field zone	Block4			Block3				Block2			Block1	
	(0–20) cm											
	Preplant	Farmer	VRT	Farmer	VRT	Preplant	VRT	Preplant	Farmer	VRT	Farmer	Preplant
Upper	C	C	C	C	C	SC	C	C	C/CL	C/CL	CL	C
Middle	C	C	C	SCL	CL/SCL	SC/CL	CL	SC/SCL	SC/CL/SCL	SCL	L	SC/SCL
Lower	CL	C	CL	C	C	C	C	C	C	C	C	C
	(20–40) cm											
Upper	C	C	C	C	C	C/SC	SC	C	CL	CL	SC	SC/CL
Middle	CL	C	C	SC/SCL	CL	SCL	SCL	C	SCL	SCL	SCL	SC
Lower	C	C	CL	C	C	C	C	C	C	C	C	C

(*) The position of the sampling refers to the 2016–17 experimental design. C: clay, CL: clay loam, SCL: silty clay loam, SC: silty clay.

Table 4. Measured and simulated yields and the corresponding fertility level (where a 1 m-soil moisture profile is recorded).
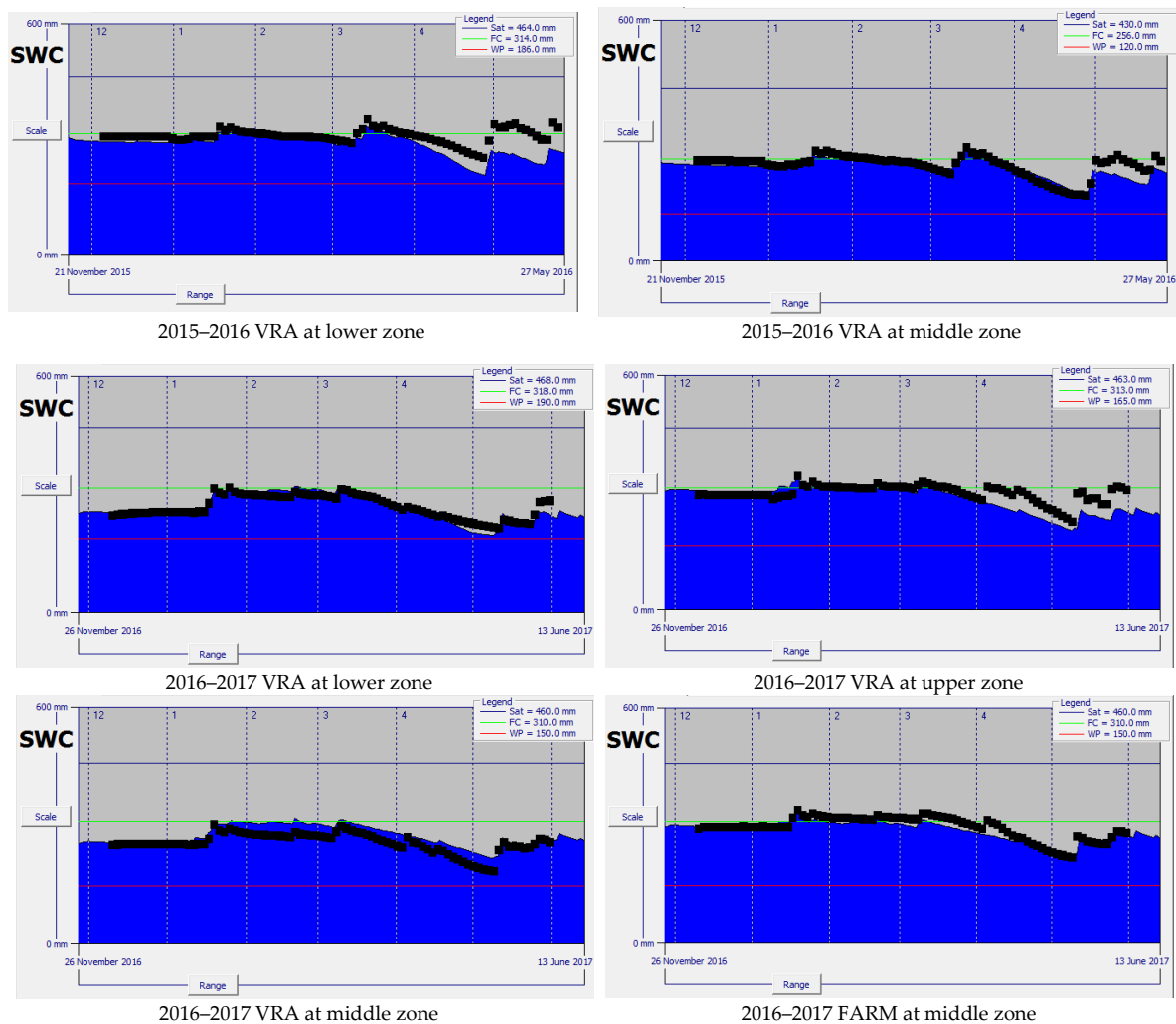
Treatment	Measured Yield (kg/ha)	Simulated Yield (kg/ha)	Fertility Level
2015–2016 VRA low	9220	8793	100%
2015–2016 VRA mid	5380	5410	59%
2016–2017 VRA low	5340	5336	72%
2016–2017 VRA mid	2070	2115	24%
2016–2017 Farm mid	1860	1835	21%
2016–2017 VRA up	3020	3010	34%

The yield simulation results during the calibration phase and the average yearly fertility using blocks 2 and 3 are presented in Table 6. The simulated yields are close to the measured ones. This indicates the high adaptation of the model and its ability to predict

the field data. In the second step, the model estimated crop yield (blocks 1 and 4) using the average soil fertility by treatment and zone during the calibration procedure. The calculated yields for the rest of the plots without soil moisture sensors in the same blocks are shown in Table 7 (validation procedure). The relative variation (%) of simulated final yields in comparison to the measured ones is presented in the Table 8. The correlation between measured and simulated yields is presented in Figure 7 and Table 9. In this table, the same correlation for the upper, middle, and lower zone is also presented.

Table 5. Simulation results (E, evaporation; T, transpiration; R, runoff; D, drainage) and Pearson correlation coefficients between measured and simulated mean daily soil water content for each 1 m profile (n = 87).

Treatment	E (mm)	T (mm)	R (mm)	D (mm)	R
2015–2016 VRA low	43	250.2	32.6	39.8	0.58
2015–2016 VRA mid	77.7	201.8	22.7	52.9	0.82
2016–2017 VRA low	106.7	216.1	12.8	8.2	0.95
2016–2017 VRA mid	162	134.4	15.2	16	0.89
2016–2017 Farm mid	168.8	120.5	15.7	57.1	0.94
2016–2017 VRA up	118.5	206.3	30.3	0	0.82

2015–2016 VRA at lower zone

2015–2016 VRA at middle zone

2016–2017 VRA at lower zone

2016–2017 VRA at upper zone

2016–2017 VRA at middle zone

2016–2017 FARM at middle zone

Figure 6. Observed (black line) and simulated (blue area) soil water content of 1 m profile.

Table 6. Results of calibration simulations (kg/ha) using fertility as adjustment parameter. Average fertility for each zone treatment (Blocks 2 and 3).

|		Lowland				Slope				Upland			
2015–2016 Cult. Per.	Treatment	Yield Meas	Fertility	Yield Sim	Average Fertility	Yield Meas	Fertility	Yield Sim	Average Fertility	Yield Meas	Fertility	Yield Sim	Average Fertility
Block2	Preplant [a]	7700	86%	7730	81%	5150	56%	5140	70%	7010	77%	7050	72%
Block3	Preplant [a]	6920	76%	6930		7560	84%	7530		6110	67%	6160	
Block2	Farmer [a]	6380	69%	6320	79%	4290	46%	4320	61%	6380	70%	6410	66%
Block3	Farmer [a]	7910	89%	7930		6720	75%	6780		5690	62%	5720	
Block2	VRA [a]	9220	100% *	8790	90%	5380	59% *	5410	78%	6700	74%	6760	75%
Block3	VRA [a]	7190	79%	7170		8520	97%	8540		6890	75%	6870	
2016–2017 Cult. Per.	Treatment	Yield meas.	Fertility	Yield sim	Average Fertility	Yield meas.	Fertility	Yield sim	Average Fertility	Yield meas.	Fertility	Yield sim	Average Fertility
Block2	Preplant [b]	4380	53%	4360	53%	3210	37%	3220	32%	2780	30%	2720	27%
Block3	Preplant [b]	4190	52%	4210		2400	27%	2400		1990	23%	2020	
Block2	Farmer [b]	4510	57%	4600	55%	1860	21% *	1840	27%	3500	40%	3480	33%
Block3	Farmer [b]	4350	53%	4360		2860	32%	2870		2210	25%	2210	
Block2	VRA [b]	5340	72% *	5370	63%	2070	24% *	2120	27%	2960	34% *	2910	39%
Block3	VRA [b]	4440	54%	4440		2700	30%	2690		3810	45%	3850	

NB 1. * Position of recorded 1 m soil moisture profile. In all other positions, only a sensor at 30 cm was installed. NB 2. Average fertility per treatment (Blocks 2 and 3): [a] 2015–2016, Preplant = 74.33%, Farmer = 68.67%, VRA = 81.00; [b] 2016–2017, Preplant = 37.33%, Farmer = 38.33%, VRA = 43.00%.

Table 7. Results of validation simulations (kg/ha) using average yearly fertility per treatment and zone (*) obtained in the calibration stage (Blocks 1 and 4).

		Lower Zone			Middle Zone			Upper Zone		
2015–2016 Cult. Per.	**Treatment**	**Yield meas**	**Fertility ***	**Yield sim**	**Yield meas**	**Fertility ***	**Yield sim**	**Yield meas**	**Fertility ***	**Yield sim**
Block1	Preplant	4990	81%	7340	5920	70%	6410	4390	72%	6610
Block4	Preplant	6270		7340	6350		6410	6680		6610
Block1	Farmer	6090	79%	7170	3370	61%	5610	5860	66%	6060
Block4	Farmer	5610		7170	7920		5620	6260		6060
Block1	VRA	7470	90%	8070	3630	78%	7030	5990	75%	6870
Block4	VRA	7190		8070	8870		7120	5880		6870
2016–2017 Cult. Per.	**Treatment**	**Yield meas**	**Fertility ***	**Yield im**	**Yieldmeas**	**Fertility ***	**Yield sim**	**Yieldmeas**	**Fertility ***	**Yield sim**
Block1	Preplant	3200	53%	4360	1220	32%	2970	1740	27%	2410
Block4	Preplant	4000		4360	2750		2990	2950		2410
Block1	Farmer	3320	55%	4440	3280	27%	2400	2870	33%	2940
Block4	Farmer	4110		4440	4170		2420	3210		2940
Block1	VRA	4670	63%	4990	2610	27%	2420	2900	39%	3260
Block4	VRA	3740		4990	4130		2420	3020		3260

Table 8. Relative variation in simulated final yield.

2015–2016 Growing Season	Treatment	Variation in Simulated vs. Measured Yield (%)		
		Lower Zone	Middle Zone	Upper Zone
Block1	Preplant	+47.09	+8.28	+50.57
Block4	Preplant	+17.07	+0.94	−1.05
Block1	Farmer	+17.73	+66.47	+3.41
Block4	Farmer	+27.81	−29.04	−3.19
Block1	VRA	+8.03	+93.66	+14.69
Block4	VRA	+12.24	−19.73	+16.84
2016–2017 Growing Season				
Block1	Preplant	+36.25	+143.44	+38.51
Block4	Preplant	+9.00	+8.73	−18.31
Block1	Farmer	+33.73	−26.83	+2.44
Block4	Farmer	+8.03	−1.97	−8.41
Block1	VRA	+6.85	−7.28	+12.41
Block4	VRA	+33.42	−41.40	+7.95
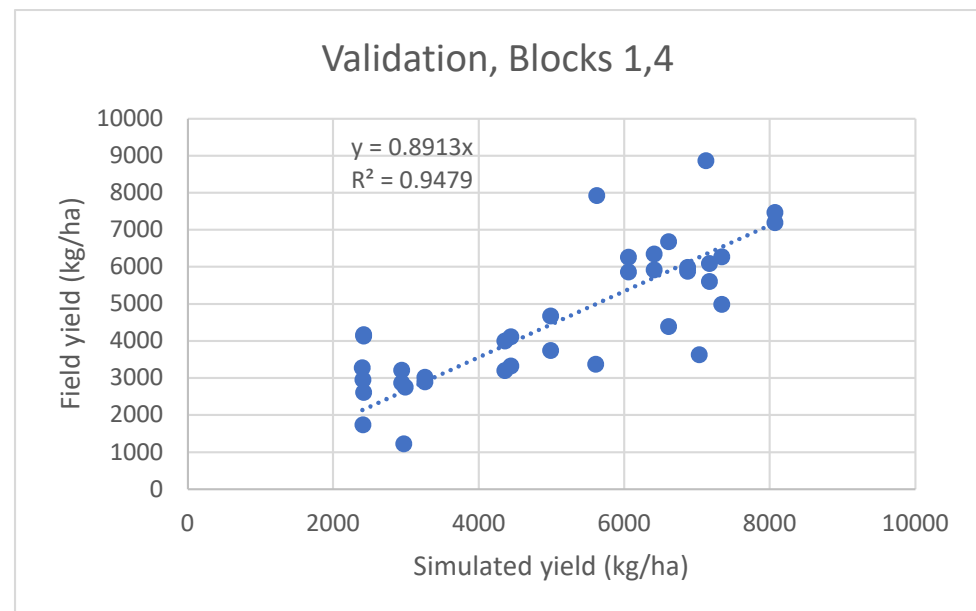
Figure 7. Field versus simulated yield for the plots selected for validation.

Table 9. Correlation of measured (y) and simulated (x) yields.

| Data	Equation	R^2
Total Field	y = 0.8913x	0.95
Upper Zone	y = 0.9059x	0.98
Middle Zone	y = 0.9666x	0.89
Lower Zone	y = 0.8358x	0.99

The statistical analysis of the data used for validation (Table 7) revealed a strong relationship between measured yield and fertility, simulated yield and fertility, and measured yield and simulated yield (Table 10).

In the following Figure 8a–d, the fertility factor and the measured yields for the three zones and the three treatments are presented.

Table 10. Correlation coefficients matrix.

	Yield Measured	**Fertility Factor %**	**Yield Simulated**
Yield measured	1.0000	0.9718 ***	0.9736 ***
Fertility factor %		1.0000	0.9990 ***
Yield simulated			1.0000

*** Correlations were significant at the 0.001 level ($p < 0.001$).
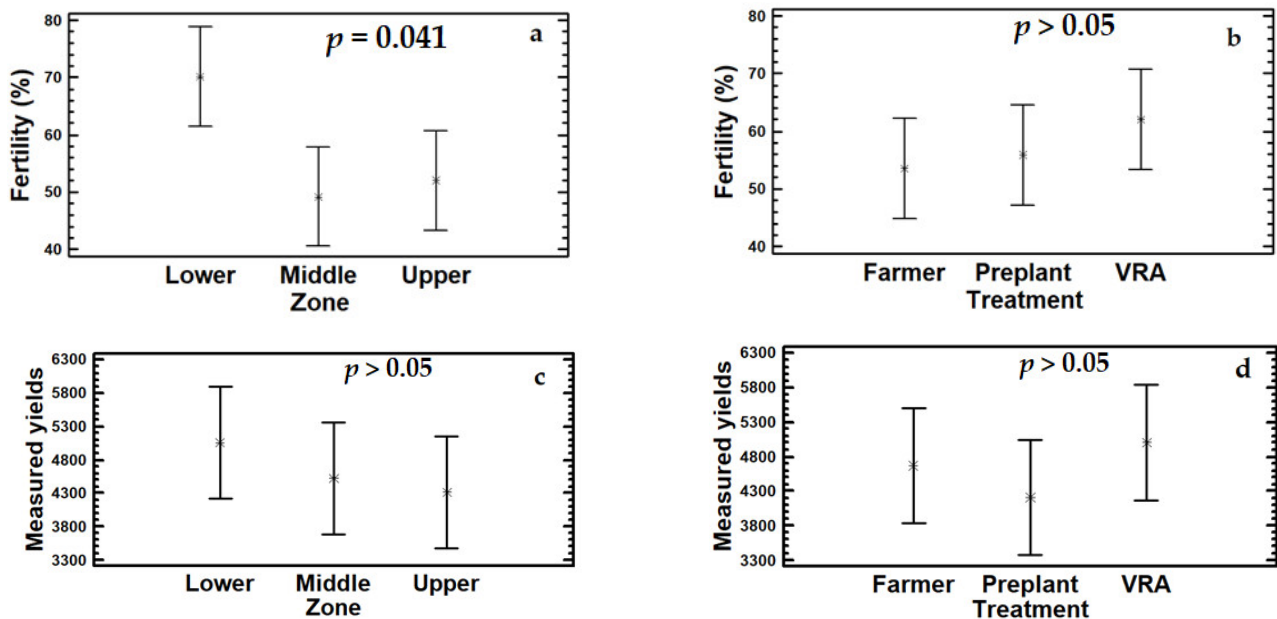
Figure 8. Fertility factor in the three zones of the field (%) and for the three treatments (%), respectively (**a**,**b**). Measured yields for the three field zones (kg/ha) and for the three treatments (kg/ha), respectively (**c**,**d**).

4. Discussion

4.1. Simulations Using the 100 cm Soil Moisture Profile

In most cases, the simulated soil water content was in agreement with the water content measured in the rootzone (Figure 6). The success of the model in simulating soil water changes was also evident by the correlation coefficients between simulated and measured moisture values in each soil profile (Table 5). Water balance parameters, such as water requirement (actual evapotranspiration), leaching, and runoff, are needed for scheduling irrigation and fertilization so that N losses can be avoided (Table 5).

Considering the field and simulated data in blocks 2 and 3, the use of VRA resulted in high fertility for the first growing season (100% in the lowland and 59% in the slope, Table 4). On the contrary, the lower N rates of the 2016–17 growing season resulted in lower soil fertility for the VRA operation (72% in lowland, 34% in upland, and 24% in the slope). Soil fertility in the slope of the farmer treatment was even lower (21%).

The actual soil fertility (expressed as a percentage of the maximum that could be achieved in Equation (2)) was used for the estimation of simulated yield. Measured yields were higher in 2016 than 2017 when comparing areas with similar conditions, i.e., lower and middle zones of VRA treatment (Table 3). This is probably due to the January 2017 frost (Figure 4a), the lower precipitation (Figure 4b,c), and the lower preplant fertilization during the second growing season. The first growing season (2015–2016) was favored by the high rainfall of March 2016 at a suitable time for plant growth. In the second year, the combination of unfavorable weather and lower preplant fertilization halted crop development, as it is seen in the fractioning of evapotranspiration. Where there was lower plant development, evaporation was higher than transpiration (Table 5).

It is also noted that the model responded to the different locations of the field. This is imprinted on yields with corresponding fertility adjustments in both growing seasons. Fertility was higher in the lower zone than in the middle and upper zone (Table 4). The higher yields in the lower zone were due to sediment accumulation and deeper and more fertile soil with higher organic matter content and greater mineralization potential. In the middle and upper zones, the fertility was lower as conditions are less favorable (increased erosion, stony and shallow soil). When comparing treatments, the VRA yields were 280 kg/ha higher than those of the conventional farmer practice by taking into consideration the middle zone of 2016–17 (Table 4).

We also observed that drainage losses were reduced, so the local environment is safe from nitrate contamination. Only in the case of the middle zone 2015 and 2016, the leaching reached up to 53–57 mm and was probably caused by lower clay content that allowed the increased infiltration of water (Table 5).

There is some concern about surface runoff, so care must be taken to avoid fertilizer application prior to big storms. The warning concerns even slightly sloped clay soil of lowland areas of the field that may have considerable runoff (Table 5).

4.2. Simulations in All the Zones of the Field for Yield Estimation

During the calibration procedure, the average fertility by treatment and zone was estimated using data from blocks 2 and 3 (Table 6). As expected, the fertility was higher in the lower zone in both growing seasons due to a deeper soil profile with fine soil texture. The fertility of the middle and upper zones was also higher in 2015–2016 (61–78%) than in 2016–17 (27–39%).

The values of simulated and measured yields during the calibration procedure (Table 6) demonstrate the ability of AquaCrop to be adapted to the field results.

Fertility stress, explaining the lower-than-potential observed yields, changed the ranking of several plots. Plots that were expected to give high yields due to their hydraulic properties and nitrogen treatment in reality appeared with a fertility much lower than the optimal. This is partially indicated by the high calcium content of the middle and upper zone [50].

The results show that yield variations were caused mostly by pedoclimatic conditions. The fertility parameter helped us exclude these external factors for a clear comparison of fertilization treatments. The comparison shows that the conventional farmer fertilization was ineffective. In Blocks 2 and 3, the fertility of farmer treatment (average value) was lower than that of the preplant in all zones of 2015–16 and in the middle zone of 2016–17 (Table 6). The results indicate that large amounts of nitrogen were lost to the environment.

Variable-rate application performed better than the other treatments in almost all cases (Table 6). In the first growing season, the VRA yields of the lower zone were 12% and 15% higher than those of the preplant and farmer treatments, respectively (Blocks 2 and 3). In the second growing season, the VRA yields of the lower zone were 14% and 10% higher than those of the preplant and farmer treatments, respectively. The fact that the higher fertility levels were achieved with less fertilizer indicates that VRA was effective as a means of targeted nitrogen application.

Taking into account the average fertility by zone and treatment (**calibration procedure** in Blocks 2 and 3), the model was applied to the corresponding plots of Blocks 1 and 4 (**validation procedure**, Table 7). The relationship between the obtained simulated yields and the measured field yields is presented in Figure 7. Regression analysis showed that this relationship is strongly linear with $R^2 = 0.95$ (Table 9). In the same table, we can observe that the model slightly overestimated the yields for all field zones. Additionally, the relationship between simulated and measured yields was stronger in the lower ($R^2 = 0.99$) and upper ($R^2 = 0.98$) zones compared to the relationship in the middle zone ($R^2 = 0.89$), probably due to its higher spatial variability (Table 9). The correlations between simulated and measured grain yield are consistent with those obtained in other studies. For example, similar values were obtained by Akumaga et al., 2017 [46]: $R^2 = 0.93$; Abedinpour et al.,

2012 [25]: R^2 = 0.96; Mebane et al., 2013 [66]: R^2 = 0.96; and Shrestha et al., 2013 [26]: R^2 = 0.90. Although the correlation coefficients were high, the range of relative variations observed in the various field zones is important: +6.85% to +47.09% in the lower zone, −41.97% to +143.44% in the middle zone, −18.31% to +50.57% in the upper zone (Table 8). The yield simulations were more successful in the lower zone.

The fertility factor was significantly higher in the lower zone (p = 0.041) (Figure 8a) reflecting the more favorable conditions for crop growth. The fertility factor did not significantly differ between the three treatments (p > 0.05) (Figure 8b). The fertility level was lower in the second growing season possibly due to less preplant fertilizer applied. The early-season frost probably contributed to the lower yields in 2017.

The measured yields were also higher in the lower zone but did not differ significantly from those obtained in the other zones (p > 0.05, Figure 8c). The measured yields did not differ significantly between the three N treatments (p > 0.05, Figure 8d). However, the lower fertilizer rate of VRA (131 kg/ha) in comparison to the farmer practice (212 kg/ha) led to a clear advantage of this technology in terms of improved fertilizer management and protection of the environment. The VRA was more effective under the favorable conditions of the low zone (deeper and more fertile root zone) and in the first growing season. The preplant N treatment was more efficient than the farmer practice.

5. Conclusions

The model was focused on the water factor and successfully simulated the evolution of soil moisture during the growing season, the estimation of the various water balance parameters, and the expected yield. The model was useful for scheduling irrigation and controlling fertilizer losses through leaching and surface runoff.

The irrigation schedule, soil texture, underground water (if any), initial soil moisture conditions, adjustment of curve number according to the slope variation, and the management practices (use of mulch or not) were needed to estimate the evolution of soil moisture during the growing season. It is important to note that the soil water content profile was close to the measured profile in most simulations, which is a strong indication of a good estimate of the water balance at the field level.

AquaCrop allows the impact of climatic conditions to be dissociated from soil fertility. It is evident that the VRA treatment increased soil fertility with a reduced nitrogen rate (81 kg N/ha less than that of the farmer in 2015–2016) and was more effective in the lower zone.

Based on the analysis of the experimental data, the ability of AquaCrop to estimate wheat yield was demonstrated in a field with high soil and topographic variability. The analysis showed the potential of AquaCrop to be adapted to the field data (calibration procedure) and its ability to give a good estimation (high R^2) of the measured yield at the field level (validation procedure). However, simulated yields with significant deviations from the real yields could be locally observed.

The water-driven AquaCrop model was proven particularly useful in optimizing agricultural practices regarding the combined effect of water and nitrogen fertilization. Analyses of this type are particularly useful for areas such as Thessaly, which has environmental issues from intense agricultural activity. The significant falls in the aquifer level, salinization, but also contamination by agrochemicals are important problems that must be addressed with the restructuring of crop patterns and the improvement of agricultural practices. AquaCrop can also help analyze the combined action of water fertilization in the context of climate change.

The weakness of the model is the qualitative approach of soil fertility. The level of fertility should be determined by experiments in the study area and/or by historic yield with corresponding fertilization data.

The model appears to be an efficient tool for evaluating and improving the management practices. To catch up with market and environmental challenges, concerted action is needed that includes improved decision-making supported by scientific evidence. More

field trials are required to verify our findings in different fields, crops, and growing seasons in the study region.

References

1. Köppen, W. Das geographische System der Klimate [The geographic system of climates]. In *Handbuch der Klimatologie*; Verlag von Gebrüder Borntraeger: Berlin, Germany, 1936.
2. Steduto, P.; Hsiao, T.; Fereres, E.; Raes, D. *Crop Yield Response to Water*; FAO Paper No. 66; FAO: Rome, Italy, 2012.
3. Doorenbos, J.; Kasssam, A.H. *Yield Response to Water*; FAO Irrigation and Drainage Paper No. 33; FAO: Rome, Italy, 1979.
4. Steduto, P.; Hsiao, T.; Fereres, E. On the conservative behavior of biomass water productivity. *Irrig. Sci.* **2007**, *25*, 189–207. [CrossRef]
5. Mustafa, S.M.T.; Vanuytrecht, E.; Huysmans, M. Combined deficit irrigation and soil fertility management on different soil textures to improve wheat yield in drought-prone Bangladesh. *Agric. Water Manag.* **2017**, *191*, 124–137. [CrossRef]
6. Farahani, H.J.; Izzi, G.; Oweis, T.Y. Parameterization and evaluation of the AquaCrop model for full and deficit irrigated cotton. *Agron. J.* **2009**, *101*, 469–476. [CrossRef]
7. García-Vila, M.; Fereres, E.; Mateos, L.; Orgaz, F.; Steduto, P. Deficit irrigation optimization of cotton with AquaCrop. *Agron. J.* **2009**, *101*, 477–487. [CrossRef]
8. Geerts, S.; Raes, D.; Garcia, M.; Miranda, R.; Cusicanqui, J.A.; Taboada, C.; Mendoza, J.; Huanca, R.; Mamani, A.; Condori, O.; et al. Simulating yield response of Quinoa to water availability with AquaCrop. *Agron. J.* **2009**, *101*, 499–508. [CrossRef]
9. Geerts, S.; Raes, D.; Garcia, M.; Taboada, C.; Miranda, R.; Cusicanqui, J.; Mhizha, T.; Vacher, J. Modeling the potential for closing quinoa yield gaps under varying water availability in the Bolivian Altiplano. *Agric. Water Manag.* **2009**, *96*, 1652–1658. [CrossRef]
10. Heng, L.K.; Evett, S.R.; Howell, T.A.; Hsiao, T.C. Validating the FAO AquaCrop model for irrigated and water deficit field maize. *Agron. J.* **2009**, *101*, 488–498. [CrossRef]
11. Hsiao, T.C.; Heng, L.K.; Steduto, P.; Rojas, B.; Raes, D.; Fereres, E. AquaCrop—The FAO crop model to simulate yield response to water: III. Parameterization and testing for maize. *Agron. J.* **2009**, *101*, 448–459. [CrossRef]
12. Maniruzzaman, M.; Talukder, M.S.U.; Khan, M.H.; Biswas, J.C.; Nemes, A. Validation of the AquaCrop model for irrigated rice production under variedwater regimes in Bangladesh. *Agric. Water Manag.* **2015**, *159*, 331–340. [CrossRef]
13. Todorovic, M.; Albrizio, R.; Zivotic, L.; Abi-Saab, M.T.; Stockle, C.; Steduto, T.C. Assessment of AquaCrop, CropSyst, and WOFOST, models in the simulation ofsunflower growth under different water regimes. *Agron. J.* **2009**, *101*, 509–521. [CrossRef]
14. Rahimikhoob, H.; Sohrabi, T.; Delshad, M. Simulating crop response to Nitrogen-deficiency stress using the critical Nitrogen concentration concept and the AquaCrop semi-quantitative approach. *Sci. Hortic.* **2021**, *285*, 110194. [CrossRef]
15. Raes, D.; Steduto, P.; Hsiao, T.C.; Fereres, E. AquaCrop–The FAO crop model to simulate yield response to water: II. Main algorithms and software description. *Agron. J.* **2009**, *101*, 438–447. [CrossRef]
16. Steduto, P.; Hsiao, T.C.; Raes, D.; Fereres, E. AquaCrop—the FAO crop model to simulate yield response to water: I. Concepts and underlying principles. *Agron. J.* **2009**, *101*, 426–437. [CrossRef]
17. Vanuytrecht, E.; Raes, D.; Steduto, P.; Hsiao, T.C.; Fereres, E.; Heng, L.K.; Garcia-Vila, M.; Moreno, P.M. AquaCrop: FAO's crop water productivity and yield response model. *Environ. Model. Softw.* **2014**, *62*, 351–360. [CrossRef]

18. Vanuytrecht, E.; Raes, D.; Willems, P. Considering sink strength to modelcrop production under elevated atmospheric CO2. *Agric. For. Meteorol.* **2011**, *151*, 1753–1762. [CrossRef]

19. Vanuytrecht, E.; Raes, D.; Willems, P. Global sensitivity analysis of yield output from the water productivity model. *Environ. Model. Softw.* **2014**, *51*, 323–332. [CrossRef]

20. Vanuytrecht, E.; Raes, D.; Willems, P.; Semenov, M. Comparing climate change impacts on cereals based on CMIP3 and EU-ENSEMBLES climate scenarios. *Agric. For. Meteorol.* **2014**, *195–196*, 12–23. [CrossRef]

21. Vanuytrecht, E.; Raes, D.; Willems, P. Regional and global climate projections increase mid-century yield variability and crop productivity in Belgium. *Reg. Environ. Chang.* **2016**, *16*, 659–672. [CrossRef]

22. Stricevic, R.; Cosic, M.; Djurovic, N.; Pejic, B.; Maksimovic, L. Assessment of the FAO AquaCrop model in simulation of rainfed and supplementally irrigated maize, sugar beet and sunflower. *Agric. Water Manag.* **2011**, *98*, 1615–1621. [CrossRef]

23. Katerji, N.; Campi, P.; Mastrorilli, M. Productivity, evapotranspiration, andwater use efficiency of corn and tomato crops simulated by AquaCrop under contrasting water stress conditions in the Mediterranean region. *Agric. Water Manag.* **2013**, *130*, 14–26. [CrossRef]

24. Hussein, F.; Janat, M.; Yakoub, A. Simulating cotton yield response to deficit irrigation with the FAO AquaCrop model. *Span. J. Agric. Res.* **2011**, *9*, 1319–1330. [CrossRef]

25. Abedinpour, M.; Sarangi, A.; Rajput, T.B.S.; Singh, M.; Pathak, H.; Ahmad, T. Performance evaluation of AquaCrop Model for maize crop in a semi-arid environment. *Agric. Water Manag.* **2012**, *110*, 55–66. [CrossRef]

26. Shrestha, N.; Raes, D.; Vanuytrecht, E.; Sah, S.K. Cereal yield stabilization in Terai (Nepal) by water and soil fertility management modeling. *Agric. Water Manag.* **2013**, *122*, 53–62. [CrossRef]

27. Shirazi, S.Z.; Mei, X.; Liu, B.; Liu, Y. Estimating potential yield and change in water budget for wheat and maize across Huang-Huai-Hai Plain in the future. *Agric. Water Manag.* **2022**, *260*, 107282. [CrossRef]

28. Hassan, D.F.; Ati, A.S.; Neima, A.S. Calibration and Evaluation of AquaCrop for Maize (*Zea Mays,* L.) under Different Irrigation and Cultivation Methods. *J. Ecol. Eng.* **2021**, *22*, 192–204. [CrossRef]

29. Abrha, B.; Delbecque, N.; Raes, D.; Tsegay, A.; Todorovic, M.; Heng, L.E.E.; Vanutrecht, E.; Geerts, S.A.M.; Garcia-Vila, M.; Deckers, S. Sowing strategies for barley (Hordeum vulgare L.) based on modelled yield response towater with AquaCrop. *Exp. Agric.* **2012**, *48*, 252–271. [CrossRef]

30. Tsegay, A.; Raes, D.; Geerts, S.; Vanuytrecht, E.; Abraha, B.; Deckers, J.; Bauer, H.; Gebrehiwot, K. Unravelling crop water productivity of tef (Eragrostis Tef (Zucc.) Trotter) through AquaCrop in northern Ethiopia. *Exp. Agric.* **2012**, *48*, 222–237. [CrossRef]

31. Tsegay, A.; Vanuytrecht, E.; Abrha, B.; Deckers, J.; Gebrehiwot, K.; Raes, D. Sowing and irrigation strategies for improving rainfed tef (Eragrostis tef (Zucc.) Trotter) production in the water scarce Tigray region, Ethiopia. *Agric. Water Manag.* **2015**, *150*, 81–91. [CrossRef]

32. Adeboye, O.B.; Schultz, B.; Adekalu, K.O.; Prasad, K. Modelling of response of the growth and yield of soybean to full and deficit irrigation by using *Aquacrop*. *Irrig. Drain.* **2017**, *66*, 192–205. [CrossRef]

33. Adeboye, O.B.; Schultz, B.; Adeboye, A.P.; Adekalu, K.O.; Osunbitan, J.A. Application of the AquaCrop model in decision support for optimization of nitrogen fertilizer and water productivity of soybeans. *Inf. Process. Agric.* **2021**, *8*, 419–436. [CrossRef]

34. Andarzian, B.; Bannayan, M.; Steduto, P.; Mazraeh, H.; Barati, M.E.; Barati, M.A.; Rahnama, A. Validation and testing of the AquaCrop model under full and deficit irrigated wheat production in Iran. *Agric. Water Manag.* **2011**, *100*, 1–8. [CrossRef]

35. Mkhabela, M.S.; Bullock, P.R. Performance of the FAO AquaCrop model for wheat grain yield and soil moisture simulation in Western Canada. *Agric. Water Manag.* **2012**, *110*, 16–24. [CrossRef]

36. Singh, A.; Saha, S.; Mondal, S. Modelling irrigated wheat production using the FAO AquaCrop model in West Bengal, India, for sustainable agriculture. *Irrig. Drain.* **2013**, *62*, 50–56. [CrossRef]

37. Toumi, J.; Er-Raki, S.; Ezzahar, J.; Khabba, S.; Jarlan, L.; Chehbouni, A. Performance assessment of AquaCrop model for estimating evapotranspiration, soil water content and grain yield of winter wheat in Tensift Al Haouz (Morocco): Application to irrigation management. *Agric. Water Manag.* **2016**, *163*, 219–235. [CrossRef]

38. Islam, T.A.F.M.; Islam, S.A.K.M.; Islam, T.G.M.; Bala, S.K.; Salehin, M.; Choudhury, A.K.; Dey, N.C.; Hossain, A. Adaptation strategies to increase water productivity of wheat under changing climate. *Agric. Water Manag.* **2022**, *264*, 107499. [CrossRef]

39. Abedinpour, M. The Comparison of DSSAT-CERES and AquaCrop Models for Wheat Under Water–Nitrogen Interactions. *Commun. Soil Sci. Plant Anal.* **2021**, *52*, 2002–2017. [CrossRef]

40. Abdou, S.M.M.; Engel, B.A.; Emam, S.M.; Abd El-Latif, K.M. AquaCrop Model Validation for Simulation Wheat Productivity under Water Stress Condition, Communications. *Soil Sci. Plant Anal.* **2022**, *53*, 281–292. [CrossRef]

41. Amiri, E.; Bahrani, A.; Irmak, S.; Mohammadiyan Roshan, N. Evaluation of irrigation scheduling and yield response for wheat cultivars using the AquaCrop model in an arid climate. *Water Supply* **2021**, *22*, 602. [CrossRef]

42. Bello, Z.A.; Walker, S. Evaluating AquaCrop model for simulating production of amaranthus (Amaranthus cruentus) a leafy vegetable, under irrigation and rainfed Conditions. *Agric. For. Meteorol.* **2017**, *247*, 300–310. [CrossRef]

43. Araya, A.; Habtu, S.; Hadgu, K.M.; Kebede, A.; Dejene, T. Test of AquaCrop model in simulating biomass and yield of water deficient and irrigated barley (Hordeum vulgare). *Agric. Water Manag.* **2010**, *97*, 1838–1846. [CrossRef]

44. Araya, A.; Keesstra, S.D.; Stroosnijder, L. Simulating yield response to water of Teff (Eragrostis tef) with FAO's AquaCrop model. *Field Crops Res.* **2010**, *116*, 196–204. [CrossRef]

45. Van Gaelen, H.; Tsegay, A.; Delbecque, N.; Shrestha, N.; Garcia, M.; Fajardo, H.; Miranda, R.; Vanuytrecht, E.; Abrha, B.; Diels, J.; et al. A semi-quantitative approach for modelling crop response to soil fertility: Evaluation of the AquaCrop procedure. *J. Agric. Sci.* **2014**, *153*, 1218–1233. [CrossRef]

46. Akumaga, A.; Tarhule, A.; Yusuf, A.A. Validation and testing of the FAO AquaCrop model under different levels of nitrogen fertilizer on rainfed maize in Nigeria, West Africa. *Agric. For. Meteorol.* **2017**, *232*, 225–234. [CrossRef]

47. Holland, K.H.; Schepers, J.S. Derivation of a variable rate nitrogen application model for in-season fertilization of corn. *Agron. J.* **2010**, *102*, 1415–1424. [CrossRef]

48. European Parliament. Directive 2000/60/EC of the European Parliament and of the Council of 23 October 2000 establishing a framework for Community action in the field of water policy. *Off. J. L* **2000**, *327*, 1–90.

49. Polychronaki, E.; Douma, C.; Giourga, C.; Loumou, A. Assessing Nitrogen Fertilization Strategies in Winter Wheat and Cotton Crops in Northern Greece. *Pedosphere* **2012**, *22*, 689–697. [CrossRef]

50. Stamatiadis, S.; Schepers, J.S.; Evangelou, E.; Tsadilas, C.; Glampedakis, A.; Glampedakis, M.; Dercas, N.; Spyropoulos, N.; Dalezios, N.R.; Eskridge, K. Variable-rate nitrogen fertilization of winter wheat under high spatial resolution. *Precis. Agric.* **2018**, *19*, 570–587. [CrossRef]

51. Dercas, N.; Dalezios, N.; Evangelou, E.; Stamatiadis, S.; Glambedakis, A.; Mantonanakis, G.; Tserlikakis, N. Wheat simulation using Aqua Crop model in precision agriculture. In Proceedings of the 6th Congress on Soil and Water Resources with International Participation, Menemen, Turkey, 12–14 November 2019.

52. Bouyoukos, G.H. A recalibration of the hydrometer method for making mechanical analysis of soils. *Agron. J.* **1951**, *43*, 434–438. [CrossRef]

53. Nelson, D.W.; Sommers, L.E. Total carbon, organic carbon, and organic matter. In *Methods of Soil Analysis, Part 2*, 2nd ed.; Page, A.L., Miller, R.H., Keeney, D.R., Eds.; Academic Press: Cambridge, MA, USA, 1982; pp. 539–579.

54. Bremner, J.M.; Mulvaney, C.S. Nitrogen-total. In *Methods of Soil Analysis, Part 2, Chemical and Microbiological Properties*, 2nd ed.; Page, A.L., Miller, R.H., Keeney, D.R., Eds.; American Society of Agronomy and Soil Science Society of America, Inc.: Madison, WI, USA, 1982; pp. 595–624.

55. Thomas, G.W. Exchangeable cations. In *Methods of Soil Analysis, Part 2, Chemical and Microbiological Properties*; Series Agronomy No. 9; Page, A.L., Miller, R.H., Keeney, D.R., Eds.; ASA and SSSA: Madison, WI, USA, 1982; pp. 159–165.

56. Olsen, S.R.; Sommers, L.E. Phosphorus. In *Methods of Soil Analysis, Part 2: Chemical and Microbiological Properties*, 2nd ed.; Page, A.L., Miller, R.H., Keeney, D.R., Eds.; ASA and SSSA: Madison, WI, USA, 1982; pp. 403–430.

57. FAO. *Irrigation and Drainage Paper N. 49*; CLIMWAT, A Climatic Database; FAO: Rome, Italy, 1994.

58. Soulis, K.X.; Elmaloglou, S.; Dercas, N. Investigating the effects of soil moisture sensors positioning and accuracy on soil moisture based drip irrigation scheduling systems. *Agric. Water Manag.* **2015**, *148*, 258–268. [CrossRef]

59. Foster, T.; Brozovic, N.; Butler, A.P.; Neale, C.M.U.; Raes, D.; Steduto, P.; Fereres, E.; Hsiao, T.C. AquaCrop-OS: An open source version of FAO's crop water productivity model. *Agric. Water Manag.* **2017**, *181*, 18–22. [CrossRef]

60. Steduto, P.; Raes, D.; Hsiao, T.; Fereres, E.; Heng, L.; Izzi, G.; Hoogeveen, J. AquaCrop: A new model for crop prediction under water deficit conditions. In *Drought Management: Scientific and Technological Innovations*; López-Francos, A., Ed.; CIHEAM: Zaragoza, Spain, 2008.

61. Raes, D.; Steduto, P.; Hsiao, T.; Fereres, E. *AquaCrop Version 6.0–6.1, Reference Manual*; FAO: Rome, Italy, 2018.

62. Mabhaudhi, T.; Modi, A.T.; Beletse, Y.G. Parameterisation and evaluation of the FAO-AquaCrop model for a South African taro (Colocasia esculenta L. Schott) landrace. *Agric. For. Meteorol.* **2014**, *192–193*, 132–139. [CrossRef]

63. Allen, R.G.; Pereira, L.S.; Raes, D.; Smith, M. *Crop Evapotranspiration. Guidelines for Computing Crop Water Requirements*; FAO Irrigation and Drainage Paper No. 56; FAO: Rome, Italy; 333p.

64. United States Department of Agriculture—USDA. *Soil, Plant, Atmosphere, Water, Field & Pond Hydrology Model*; USDA Agricultural Research Service: Beltsville, MD, USA, 2007.

65. Akbari, A.; Samah, A.; Ngien, S. Effect of slope adjustment on curve number using global digital elevation data: New look into Sharply Williams and Huang Methods. In Proceedings of the Second International Conference on Science, Engineering & Environment, Osaka, Japan, 21–23 November 2016.

66. Mebane, V.J.; Day, R.L.; Hamlett, J.M.; Watson, J.E.; Roth, G.W. Validating the FAO AquaCrop model for rainfed maize in Pennsylvania. *Agron. J.* **2013**, *105*, 419–427. [CrossRef]